Brazilian Journal
of Chemical
Engineering

ISSN 0104-6632
Printed in Brazil
www.abeq.org.br/bjche

Vol. 29, No. 03, pp. 635 - 652, July - September, 2012

COMPARISON OF ADSORPTION EQUILIBRIUM AND KINETIC MODELS FOR A CASE STUDY OF PHARMACEUTICAL ACTIVE INGREDIENT ADSORPTION FROM FERMENTATION BROTHS: PARAMETER DETERMINATION, SIMULATION, SENSITIVITY ANALYSIS AND OPTIMIZATION

B. Likozar[1*], D. Senica[2] and A. Pavko[3]

[1]Laboratory of Catalysis and Chemical Reaction Engineering, National Institute of Chemistry,
Phone: + 386 1 4760 282, Fax: + 386 1 4760 300, Hajdrihova 19, SI 1000 Ljubljana, Slovenia.
E-mail: blaz.likozar@ki.si
[2]Lek d. d., Verovškova 57, SI 1526 Ljubljana, Slovenia.
[3]University of Ljubljana, Faculty of Chemistry and Chemical Technology, Chair of Chemical,
Biochemical and Environmental Engineering, Aškerčeva cesta, 5, SI 1000, Ljubljana, Slovenia.

(Submitted: June 8, 2011 ; Revised: December 29, 2011 ; Accepted: February 23, 2012)

Abstract - Mathematical models for a batch process were developed to predict concentration distributions for an active ingredient (vancomycin) adsorption on a representative hydrophobic-molecule adsorbent, using differently diluted crude fermentation broth with cells as the feedstock. The kinetic parameters were estimated using the maximization of the coefficient of determination by a heuristic algorithm. The parameters were estimated for each fermentation broth concentration using four concentration distributions at initial vancomycin concentrations of 4.96, 1.17, 2.78, and 5.54 g l^{-1}. In sequence, the models and their parameters were validated for fermentation broth concentrations of 0, 20, 50, and 100% (v/v) by calculating the coefficient of determination for each concentration distribution at the corresponding initial concentration. The applicability of the validated models for process optimization was investigated by using the models as process simulators to optimize the two process efficiencies.
Keywords: Pharmaceuticals; Adsorption equilibrium; Adsorption kinetics; Mathematical modeling; Optimization.

INTRODUCTION

Pharmaceutical active ingredients are usually drugs that are biologically active. They are produced in biotechnological processes and are obtained as products from fermentation broths. In order to purify these active ingredients, downstream processing is utilized. Adsorption is one of the most common unit operations involved and thus optimization of this process is usually directly related to successful product isolation and increased added value.

Vancomycin, which is a glycopeptide antibiotic along with *N*-dimethylvancomycin that is produced by the actinomycete *Amycolatopsis orientalis* (McIntyre *et al.*, 1996), was chosen as the active ingredient for this case study. Adsorption of vancomycin was studied using different adsorbents. Yan *et al.* (2000) used cross-linked poly(*N*,*N*-dimethylacrylamide) with the

*To whom correspondence should be addressed

immobilized peptidoglycan analogues -aminolevulinic acid-aminolevulinic acid, -succinyl-aminolevulinic acid and -succinyl-glycine, while Yuan *et al.* (2001) used cross-linked polyacrylamide with immobilized alanine. Tian *et al.* (2006, 2008) examined the adsorption on hemofilters in two consecutive studies, while von Winckelmann *et al.* (2009) utilized molecular adsorbents. Scale-up of these processes to an industrial level, however, is probably technologically not viable and therefore preliminary studies were performed by our group using relatively cost-effective polymeric adsorbents (Borin and Pavko, 2009; Likozar *et al.*, 2012).

In order to successfully simulate and optimize the adsorption of a chosen active ingredient, adsorption equilibrium and kinetic models had to be compared. Adsorption kinetic models are usually divided into two subgroups. The first ones are the non-structural models which may agree quite well with the experimental data; nonetheless, these do not include parameters describing adsorbent structure and are thus more or less of an interpolative nature. Among these are the Thomas model (Han *et al.*, 2007) and models based on the law of mass action (Moraes *et al.*, 2009; Papini *et al.*, 1999), applied to a wide range of adsorption processes of metals (Papini *et al.*, 1999), heterocyclic compounds (Han *et al.*, 2007), and enzymes (Moraes *et al.*, 2009). The second subgroup are the structural models, which usually also agree quite well with experimental data and include parameters describing adsorbent structure such as adsorbent particle size (Dadwhal *et al.*, 2009; Forrer *et al.*, 2008; Quek and Al-Duri, 2007), micro-particle size (Dadwhal *et al.*, 2009), particle size distribution (Du *et al.*, 2007) or other characteristic dimensions (Zabka *et al.*, 2006), and are thus more of an extrapolative nature. These models, however, usually have to be solved numerically as opposed to the non-structural ones, which usually take the form of a relatively simple expression or have an exact solution. The latter thus provide simple, fast, but less accurate predictions, whereas the former require more complex algorithms, their solving is time-consuming; nonetheless, the solutions obtained are relatively accurate and give more insight into the underlying mechanisms of the process.

The main objective of the present work was to develop several mathematical models to simulate concentration decrease distributions for adsorption of an active ingredient (vancomycin) onto a representative adsorbent for hydrophobic molecules, using a crude fermentation broth containing cells. The models were then validated and the best one was used to optimize the process.

MATERIALS AND METHODS

Materials

The microorganism and culture conditions were as follows. *Amycolatopsis orientalis* was employed to produce the vancomycin. The microorganism (ATCC 19795 and NCIMB 12945) is typically grown on GS (glucose/sucrose) broth. The inoculated cultures are grown on a medium containing 5% glucose, 10% soluble starch, 5% peptone, and 5% yeast extract at pH 6.7. Vancomycin is produced in 250 ml flasks containing 40 mL of culture medium (20 g L^{-1} glucose/sucrose, 5 g L^{-1} peptone, 0.75 g l^{-1} $MgSO_4 \cdot 6H_2O$, 1 g L^{-1} NaCl, 0.5 g L^{-1} KCl, 10 g L^{-1} trace metal solution and 10 g L^{-1} 3-(*N*-morpholino)propanesulfonic acid) pH 6.7, using a 5% inoculum and incubating at 30 °C in an orbital shaker at 3.7 rps for 96−120 h (McIntyre *et al.*, 1996).

The adsorbent was AMBERLITE XAD 16 N from ROHM AND HAAS (Philadelphia, USA). This resin is an adsorbent for hydrophobic molecules and the AMBERLITE XAD generation of adsorbents was especially designed for both batch and continuous adsorption, having a low density and large particle diameters between 560 and 710 μm (R_p = 0.3175 mm). R_μ was determined from scanning electron micrograms as 1.69 μm (Likozar *et al.*, 2012).

Batch Experiments

The vessels used in the batch experiments were Erlenmeyer flasks (flask volume 25−100 mL, the total volume of suspension of 24−69 mL). Comparison of the concentration distributions for different fermentation broth concentrations was made as follows. The adsorbent was first fed with distilled water (pH 7.0) and then with the culture medium containing cells at pH 6.7. The adsorption performance of the batch was compared at different fermentation broth concentrations (0, 20, 50 and 100% (v/v), with the same adsorbent porosity (0.550)) with fractions of adsorbent of 0.164−0.277, respectively. All the experiments were carried out at 21−22 °C. The system was not mechanically mixed, but rather the Erlenmeyer flasks were mixed using a laboratory shaker. The rotational frequencies used were 50 min^{-1}, 100 min^{-1}, 220 min^{-1}, 300 min^{-1}, 400 min^{-1}, 600 min^{-1} and 1000 min^{-1}. The hydrodynamic conditions for the batch process were turbulent, since the Reynolds number was approximately 1500 for the lowest rotational frequency utilized (50 min^{-1}), and, for the majority of experiments, even higher than 10^4. The vancomycin concentration was

determined in the liquid separated from the batch. The fermentation broth concentration of 0% (v/v) was obtained as the supernatant after separating all the biomass from 100% (v/v) broth using centrifugation.

Vancomycin assay (concentration) was determined by high performance liquid chromatography with a mobile phase of 100% (v/v) acrylonitrile and a 5 mM phosphate buffer pH 2.6 at a flow rate of 1 mL min^{-1}. The column (ZORBAX SB-Aq; 4.6 × 50 mm, 1.8 μm; Agilent Technologies) was maintained at 45 °C, 2 mL of antibiotic solution injected and the concentration of glycopeptide antibiotic determined with a UV–Vis (ultraviolet–visible) absorbance detector. The number of units of vancomycin concentration was determined as the amount of antibiotic that corresponded to a specific mass of the latter per volume from a calibration curve obtained under the conditions mentioned above. For the validation of the model predictions of concentration profiles two independent experimental methods were applied: the chromatographic experimental method described above and a gravimetric method. At specified times the adsorbent was removed from the vancomycin solution, dried and subsequently weighed. The adsorbed amount was calculated from the difference between neat and used adsorbent. Chromatographic and gravimetric experimental methods were comparable; nonetheless, the former was used for model regression and validation due to its higher accuracy.

THEORY AND CALCULATION

The development of a mathematical model for the batch vessel adsorption process for vancomycin purification on a hydrophobic-molecule adsorption resin was based on the following hypotheses:

(i) The antibiotic concentration at the specific location in the adsorbent pore was in local equilibrium with its concentration adsorbed on the inner surface of the pore wall at the corresponding specific location;

(ii) The hydrodynamic behavior of the liquid phase could be neglected as mixing did not have any effect on the adsorption rate (Likozar *et al.*, 2012);

(iii) The size distribution of the particles was considered to be the same or different throughout the fluidized adsorbent and the void fraction, depending on the model;

(iv) The rheological properties of the crude extract and other media were considered to be the same in all the experiments and independent of the exact concentration;

(v) The microorganism mass balance was not presented, because microorganism adsorption onto the resin was considered to be negligible. The differential mass balance in an element of the batch volume for vancomycin concentration may be due to the absence of mass transfer resistance around adsorbent particles expressed by (ε represents the volume fraction of liquid phase and ρ represents the solid density):

$$\frac{\partial C}{\partial t} = -\frac{1-\varepsilon}{\varepsilon}\rho\frac{\partial \overline{q}}{\partial t} \tag{1}$$

The initial condition is:

$$t = 0 \qquad C = C_0 \tag{2}$$

At equilibrium, the adsorption equilibrium isotherm can be represented by the Sips model (Equation (3)), which was previously reported to describe the arsenic adsorption process in batch and continuous adsorption (Dadwhal *et al.*, 2009; Yang *et al.* 2006). There are numerous other adsorption equilibrium models, e.g. Langmuir, Freundlich, Redlich–Peterson, Temkin, Dubinin–Radushkevich, etc., that can be used for biomolecules, e.g. chitosan (Gottipati and Mishra, 2010; Kumar *et al*., 2010; Piccin *et al*., 2011), but the Sips model proved to be the best for vancomycin adsorption onto polymeric resin (Likozar *et al*., 2012).

$$q^* = \frac{q_{max} C^{*n}}{K_D + C^{*n}} \tag{3}$$

Thomas Model

The data obtained in batch vessel mode studies was used to calculate the maximum gel phase concentration of vancomycin on the adsorbent and other equilibrium parameters, while the adsorption rate constant was calculated using the kinetic model developed by Thomas (1944). The Thomas model (TM) is one of the most general and widely used models in column performance theory. The modified expression of Thomas for an adsorption vessel is given as follows:

$$\frac{C}{C_0} = \exp\left(k_1\left(\frac{1-\varepsilon}{\varepsilon}\rho q^* - C_0\right)t\right) \tag{4}$$

where k_1 is the Thomas rate constant $(m^3 kg^{-1} s^{-1})$, q^* is the equilibrium vancomycin uptake per kg of the adsorbent $(q^* = \overline{q})$ (kg kg^{-1}), C_0 is the initial

vancomycin concentration (kg m^{-3}), and C is the liquid concentration at time t (kg m^{-3}).

Reversible Second Order/First Order Kinetics

The differential mass balance in the solid phase is represented according the following mathematical kinetic model (reversible second order/first order kinetics – RSFK):

$$\frac{\partial \overline{q}}{\partial t} = k_1 C\left(q_{max} - \overline{q}\right) - k_2 \overline{q} \quad (5)$$

where k_1 and k_2 are intrinsic kinetic constants, C is the vancomycin concentration in the solution, $\overline{q}$ is the antibiotic concentration adsorbed on the polymer and q_{max} is the maximum adsorption capacity of the resin. The initial condition was:

$$t = 0 \qquad \overline{q} = 0 \quad (6)$$

Reversible *n*+1-th Order/First Order Kinetics

The vancomycin adsorption data are reported in Figure 1 as a function of time at several fermentation broth concentrations. The organic molecule adsorption was formulated in the model according to the reversible n+1-th order/first order kinetics surface adsorption/desorption model (RNFK) by using the previous basic equilibrium equation (with reference to the adsorption site) (Equation (3)). The mass balance equation for the surface sites was modified to account for the vancomycin occupancy and is expressed analogously by Equation (1) which, combined with the mass action law, gave rise to the adsorption equation used to fit the experimental data.

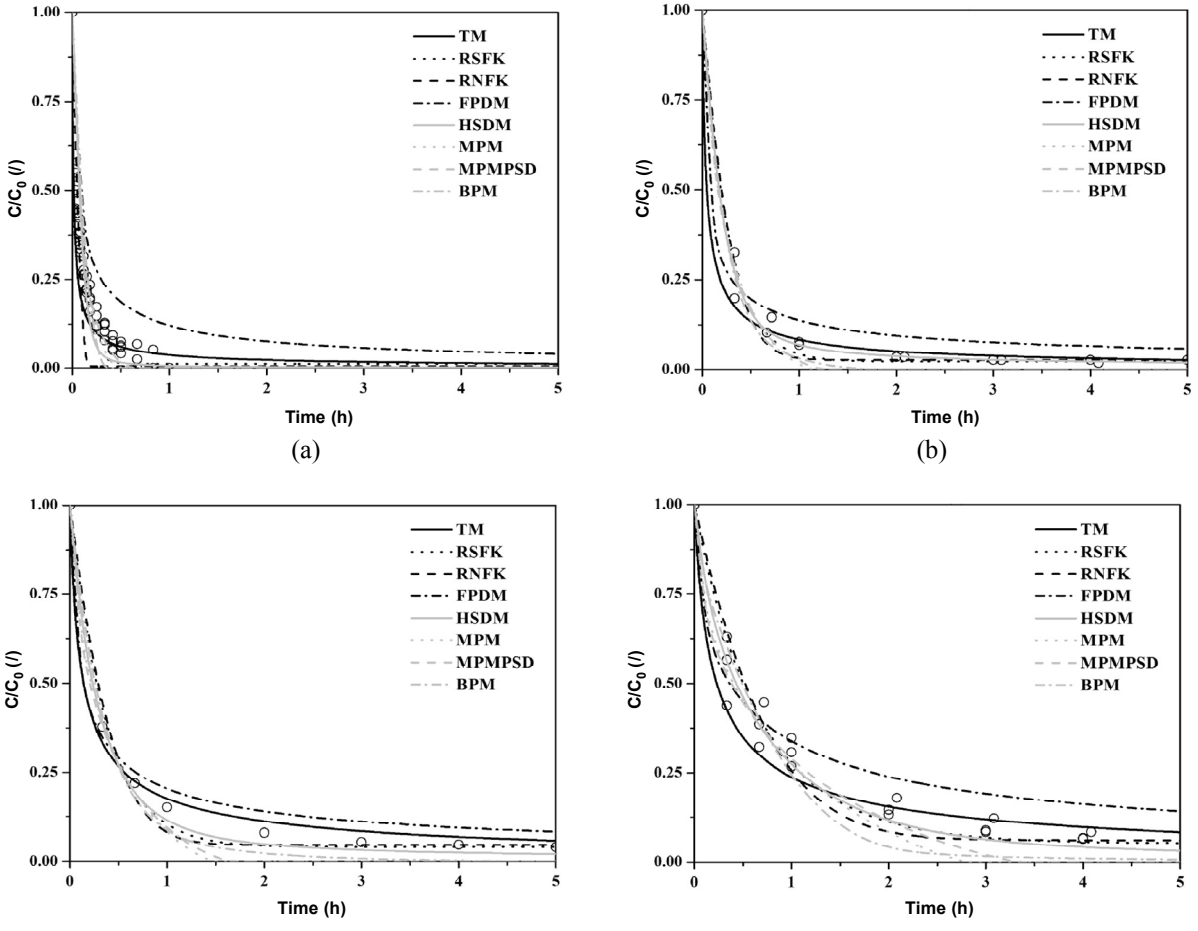

Figure 1: Concentration distributions for vancomycin adsorption in a batch vessel (validation of models). (a) FB concentration 0% (v/v) (C_0 = 4.96 g l^{-1}); (b) FB concentration 20% (v/v) (C_0 = 1.17 g l^{-1}); (c) FB concentration 50% (v/v) (C_0 = 2.78 g l^{-1}); (d) FB concentration 100% (v/v) (C_0 = 5.54 g l^{-1}).

Film–Pore Diffusion Model

The film–pore diffusion model (FPDM) of interest in this work was proposed by Spahn and Schlünder (1975) and Brauch and Schlünder (1975), based on the unreacted core theory (Levenspiel, 1999; Yagi and Kunii, 1961). This model describes the occurrence of adsorption by external film mass transfer (which may be negligible), followed by intra-particle pore diffusion to the adsorption sites where solute molecules (adsorbate) are taken up. The adsorbent particle is regarded as a porous gel. The adsorbate in the solution is adsorbed in a well-defined concentration front which starts at the outer surface of the adsorbent particles, moving radial-wise inward with a certain velocity, leaving an unadsorbed zone at the center.

A few assumptions are made for this theory, i.e, the transfer of solute molecules within the pores of an adsorbent particle occurs only by molecular diffusion, the adsorption equilibrium occurs between the pore and solute solution throughout the particle from the adsorbent surface to the concentration front, the adsorption is irreversible, and the concentration of solute molecules in the pore water is negligible compared with that on the adsorbent per unit weight.

Because of the negligibility of external mass transfer from the external liquid phase, as outlined below, diffusion in the liquid-filled pore occurs according to Fick's first law:

$$\dot{m} = \frac{4\pi D_l}{1/r_f - 1/R_p} C \tag{7}$$

The velocity of the concentration front is obtained from the mass balance on a spherical element:

$$\dot{m} = -4\pi \frac{\varepsilon}{1-\varepsilon} \rho {r_f}^2 \frac{\partial r_f}{\partial t} q^* \tag{8}$$

The average concentration in the gel is given by

$$\bar{q} = q^* \left(1 - \left(\frac{r_f}{R_p} \right)^3 \right) \tag{9}$$

Homogenous Surface Diffusion Model

The homogenous surface diffusion model (HSDM) is based on the assumption that the transport of species is determined either by external mass transfer in the liquid phase, if the latter is not negligible, or by external equilibrium between the liquid and solid phase and by intra-particle diffusion resistance in the form of surface diffusion within the adsorbent particle. Assuming homogeneous spherical adsorbent particles, a concentration-independent diffusivity (this assumption was relaxed by Yang *et al.* (2006) without offering any particular advantage in the model fit), the intra-particle transport and solute uptake is described by the following equation (Yang *et al.*, 2006):

$$\frac{\partial q}{\partial t} = \frac{D_l}{r^2} \frac{\partial}{\partial r} \left(r^2 \frac{\partial q}{\partial r} \right) \tag{10}$$

where q is the solute loading in the adsorbent phase (kg kg^{-1}), D_l is the intra-particle diffusion coefficient (m^2 s^{-1}), and r is the radial distance (m) measured from the center. The boundary and initial conditions (BC and IC) are the following:

$$t = 0 \quad q = 0 \tag{11}$$

$$r = 0 \quad \frac{\partial q}{\partial r} = 0 \tag{12}$$

$$r = R_p \quad q = q^* \tag{13}$$

At the external surface of the particle $(r = R_p)$, instantaneous equilibrium is assumed between the organic molecule concentrations in the liquid and solid phases, which are coupled using the Sips isotherm, as obtained from the adsorption equilibrium experiments (see discussion below).

$$q^* = \frac{q_{max} C^n}{K_D + C^n} \tag{14}$$

The average solute concentration in the adsorbent particle is defined as:

$$\bar{q} = \frac{3}{{R_p}^3} \int_0^{R_p} q r^2 dr \tag{15}$$

Mono-Disperse Pore Model

The corresponding mass balance for the stagnant liquid in the particle pores for the mono-disperse pore model (MPM) can be written as:

$$\frac{\partial C_m}{\partial t} = -\frac{1-\varepsilon_m}{\varepsilon_m}\rho\frac{\partial q^*}{\partial t} + \frac{D_l}{r^2}\frac{\partial}{\partial r}\left(r^2\frac{\partial C_m}{\partial r}\right) \quad (16)$$

where C_m is the pore concentration of the component, q^* the corresponding concentration in the gel phase, D_l the diffusivity of component and R_p the radial position. It must be noted that, according to the previous definition, $t = 0$ corresponds to the time of a component being totally excluded from the pores. A detailed description of nomenclature, BC, IC and the calculation of $\bar{q}$ for $\bar{q}_\mu = q^*$ is presented later.

Monodisperse Pore Model with Particle Size Distribution

The particle diameters of the macro-porous resin AMBERLITE XAD 16N used here may be considered to be non-uniform. Therefore, variations of the particle size distribution may be considered. The particle size (radius) distribution for spherical particles is approximately expressed by a normal (Gaussian) distribution (Yun *et al.*, 2004):

$$f\left(R_p\right) = \frac{1}{\sqrt{2\pi}\sigma_s}\exp\left(-\frac{\left(R_p - R_p^{mean}\right)^2}{2{\sigma_s}^2}\right) \quad (17)$$

where R_p^{mean} and σ_s are the average radius and standard deviation of the particles. Since there are 2.0% particles in each size range $R_p < R_{p,min}$ or $R_p > R_{p,max}$ and the uniformity coefficient is 2.0, Equation (17) has been modified along these lines, the mean diameter being 0.3175 mm and the diameter variance being 1.9257×10^{-2} mm^2. Equation (17) fulfills the following condition:

$$\int_{-\infty}^{\infty} f\left(R_p\right)dR_p = 1 \quad (18)$$

To simulate concentration profiles with the particle size distribution (PSD), the PSD was approximated by a discrete distribution. The interval between $R_{p,min}$ and $R_{p,max}$ was divided into 18 fractions (the additional two fractions being $R_p < R_{p,min}$ and $R_p > R_{p,max}$). The value of the discrete probability density distribution for each fraction was calculated from the integral:

$$\bar{f}\left(R_{p,i}^{average}\right) = \int_{R_{p,i}}^{R_{p,i}+\Delta R_p} f\left(R_p\right)dR_p \quad (19)$$

where

$\Delta R_p = \left(R_{p,max} - R_{p,min}\right)/18$ and

$R_{p,i}^{average} = R_{p,i} + \Delta R_p/2$.

With the consideration of the impact of the particle size distribution, the general rate for the monodisperse pore model with particle size distribution (MPMPSD) consists of two differential mass transport equations (Du *et al.*, 2007) for the liquid phase mass balance (Equation (1)) and the stationary phase mass balance ($C_{m,i}$ is the solute concentration in the pores of the *i*-th particle fraction):

$$\frac{\partial C_{m,i}}{\partial t} = -\frac{1-\varepsilon_m}{\varepsilon_m}\rho\frac{\partial q_i^*}{\partial t} + \frac{D_l}{r^2}\frac{\partial}{\partial r}\left(r^2\frac{\partial C_{m,i}}{\partial r}\right) \quad (20)$$

with the initial and boundary conditions:

$$t = 0 \quad C_{m,i} = 0 \quad (21)$$

$$r = 0 \quad \frac{\partial C_{m,i}}{\partial r} = 0 \quad (22)$$

$$r = R_p \quad C_{m,i} = C \quad (23)$$

where q_i^* is the concentration in the gel phase of the particle (kg kg^{-1}), C is the concentration in the stagnant liquid phase (kg m^{-3}), D_l is the effective diffusivity (m^2 s^{-1}), and ε_m the particle porosity. A detailed description of the calculation of $\bar{q} = \sum_i \bar{f}\left(R_{p,i}^{average}\right)\bar{q}_i$ and substituting for $\bar{q}_\mu = q_i^*$, $C_m = C_{m,i}$, and $\bar{q} = \bar{q}_i$ is presented later.

Bidisperse Pore Model

The bidisperse pore model (BPM) assumes that the adsorbent particle is an agglomerate of a number of equal sized micro-particles. A porous inter-gel region forms in between the micro-particles. Before the organic molecule adsorbs inside the micro-particle, it must be transported from the particle surface through the inter-gel region to the surface of

the micro-particles. In the inter-gel porous region, transport is described by the following equation (Cen and Yang, 1986; Yang *et al*., 2004):

$$\frac{\partial C_m}{\partial t} = -\frac{1-\varepsilon_m}{\varepsilon_m}\rho\frac{\partial \overline{q}_\mu}{\partial t} + \frac{D_l}{r^2}\frac{\partial}{\partial r}\left(r^2\frac{\partial C_m}{\partial r}\right) \tag{24}$$

The BC and IC are the following:

$$t = 0 \quad C_m = 0 \tag{25}$$

$$r = 0 \quad \frac{\partial C_m}{\partial r} = 0 \tag{26}$$

$$r = R_p \quad C_m = C \tag{27}$$

where C_m is the solute concentration in the inter-gel porous region (kg m^{-3}), $\overline{q}_\mu$ is the volume-averaged solute concentration in the solid phase (micro-particles) (kg kg^{-1}) – see Equation (33) below – R_p is the particle external radius (m). D_l is the inter-gel porous region diffusivity (m^2 s^{-1}), given by $(\varepsilon_m / \Gamma)D_b$ with ε_m being the void fraction in the porous region, Γ, the tortuosity, and D_b, molecular diffusivity.

Transport and adsorption in the micro-particles are described by

$$\frac{\partial q_\mu}{\partial t} = \frac{D_\mu}{r_\mu^{\,2}}\frac{\partial}{\partial r_\mu}\left(r_\mu^{\,2}\frac{\partial q_\mu}{\partial r_\mu}\right) \tag{28}$$

with the BC and IC being:

$$t = 0 \quad q_\mu = 0 \tag{29}$$

$$r_\mu = 0 \quad \frac{\partial q_\mu}{\partial r_\mu} = 0 \tag{30}$$

$$r_\mu = R_\mu \quad q_\mu = \frac{q_{max} C_m^{\,n}}{K_D + C_m^{\,n}} \tag{31}$$

where q_μ is the solute concentration (kg kg^{-1}) in the micro-particle, D_μ is the micro-particle diffusivity (m^2 s^{-1}), and R_μ is the micro-particle radius (m). Equation (31) is the Sips isotherm, which has been shown experimentally to describe vancomycin adsorption in the macro-reticular cross-linked poly(divinylbenzene) adsorbent (see above). The average concentration throughout the adsorbent particle is defined as:

$$\overline{q} = \frac{3}{\rho R_p^{\,3}}\int_0^{R_p} r^2\left(\rho\overline{q}_\mu + \frac{\varepsilon_m}{1-\varepsilon_m}C_m\right)dr \tag{32}$$

where $\overline{q}_\mu$ is given by:

$$\overline{q}_\mu = \frac{3}{R_\mu^{\,3}}\int_0^{R_\mu} q_\mu r_\mu^{\,2} dr_\mu \tag{33}$$

The partial differential equation presented as Equation (1) was numerically solved using the fourth-order Runge–Kutta or explicit finite difference discretization methods, which led to a (system of) linear equation(s), numerically solved by the MATLAB R2009b routines. Equation (1) became an ordinary differential equation when all dependent variables could be expressed only as a function of time (depending on the model; specifically, the first four models). The differential mass balances in the gel phase (Equations (5), (7), (8), (10), (16), (20), (24), and (28)) were solved in the (space)–time domain using the MATLAB R2009b routines for each time step as well. The parameters of the models, namely k_1, k_2, D_l and D_μ were estimated using an iterative method, that is MCOD (the maximization of the coefficient of determination).

The MCOD version used in this study was based on an algorithm that examined the coefficients of determination over the search interval and then continuously narrowed this interval until the global maximum of the coefficient of determination was found using the three-digit accuracy of a parameter as the termination condition. The search intervals for the model parameters were defined according to physical limitations and the parameters were allowed to vary as follows: $k_1 / (l^n g^{-n} h^{-1}) \in [10^{-20}, 10^{20}]$, $k_2 / (h^{-1}) \in [10^{-20}, 10^{20}]$, $D_l / (m^2 s^{-1}) \in [10^{-5}, 10^{-20}]$, and $D_\mu / (m^2 s^{-1}) \in [10^{-5}, 10^{-20}]$. The rationale for using the search intervals of 40 orders of magnitude was as follows. The aim was to find globally and not just locally the optimal values of the process model parameters. If the search intervals were narrowed, the optimal local values would have been obtained faster in terms of computational time; nonetheless, the actual optimal global values could have been outside of the utilized search intervals. Since maximally two

parameters were regressed simultaneously, the performance of regression analysis was not poor in terms of computational time.

The estimation of the parameters thus consisted of maximizing the coefficient of determination (COD) described by Equation (34), where *y* is the vector of the experimental concentration distributions and y^{calc} is the vector calculated by the model ($\overline{y}$ and $\overline{y}^{calc}$ are the averages of both vectors). The applied parametric search algorithm was the Levenberg–Marquardt algorithm using the tolerance of 10^{-5}. For different regression analysis cycles, uniformly distributed pseudorandom numbers were multiplied by the search intervals to determine the starting points of the parameters applied in the search algorithm. After several cycles the parameter values yielding the highest COD were singled out as optimal.

$$COD = \frac{\sum_{i=1}^{n}\left(y_i - \overline{y}\right)\left(y_i^{calc} - \overline{y}^{calc}\right)}{\sqrt{\sum_{i=1}^{n}\left(y_i - \overline{y}\right)^2}\sqrt{\sum_{i=1}^{n}\left(y_i^{calc} - \overline{y}^{calc}\right)^2}} \qquad (34)$$

Four complete concentration distributions were employed in the estimation of the parameters at fixed concentrations (4.96, 1.17, 2.78, and 5.54 g L^{-1}) for four fermentation broth (FB) concentrations: 0, 20, 50 and 100% (v/v).

RESULTS AND DISCUSSION

Determination of Adsorption Isotherms and Kinetics

A common practice in the modeling of adsorption processes is the use of the kinetic parameters (k_1 (and k_2) or D_l, (and D_μ)) and the equilibrium parameters for the capacity, reciprocal constant, and order (q_{max}, K_D, (and n)) estimated by nonlinear regression, besides empirical correlations to calculate the transport parameters (liquid phase mass transfer around adsorbent particles was negligible in our case (Likozar *et al.*, 2012)) and batch properties (porosity) in order to simulate the process in a batch. In most cases, the model shows good performance, fitting the experimental data well. However, this is often not applicable to the use of crude broth for active ingredient adsorption in a batch since previous simulations showed several deviations between the model and the experimental data, because the fermentation broth concentration was not accounted for.

As an illustration, the parameters of the previous study of Burkert *et al.* (2006), who reported adsorption data for inulinase in a stirred tank employing a specific resin, constant pH and temperature, were used to simulate the adsorption of inulinase in an expanded bed under the same conditions (Moraes *et al.*, 2009). The column efficiencies calculated from the model breakthrough curve prediction and from the experimental data were 74.0% and 57.3%, respectively (Moraes *et al.*, 2009). This result shows that the best alternative was to re-estimate the model parameters employing experimental data collected in an expanded bed. Chang and Chase (1996) had previously reported that the correlations in the literature did not correlate well with experimental data in expanded beds.

The estimation of the parameters was carried out using four concentration distributions for vancomycin adsorption from fermented broth containing cells in an AMBERLITE XAD 16 N adsorbent batch. The complete concentration distributions, which are referred to as FB 0, 20, 50 and 100% (v/v), were obtained as the experimental data. The effect of the rotational velocity (ω_r) was first taken into consideration for the hydrodynamic behavior study, its values being 50 min^{-1}, 100 min^{-1}, 220 min^{-1}, 300 min^{-1}, 400 min^{-1}, 600 min^{-1} and 1000 min^{-1} for FB concentrations of 0, 20, 50 and 100% (v/v), respectively. The concentration distributions did not differ for variable rotational velocities and thus liquid phase mass transfer around adsorbent particles could be considered to be negligible (Likozar *et al.*, 2012).

Ideally, only one set of optimal parameters would exist, but unfortunately realistic data reduction cannot yield a single set of parameters, even using a method for parameter estimation with global characteristics, such as MCOD. The estimated parameters are presented in Tables 1 and 2 for each FB concentration investigated. In all cases, the estimated parameters were of similar order of magnitude, mainly for q_{max}, n, and D_l. The confidence intervals of the individual parameters in Table 2 in terms of parameter standard deviation (σ) were calculated as $\sigma^2 = \left(J^T J\right)^{-1} \sum_{i=1}^{N}\left(y_i - y_i^{calc}\right)^2 \Big/ \left(N - p\right)$, where J is the Jacobian matrix of the minimized function at the solution (optimal parameters), while N and p are the numbers of measurements and parameters.

Table 1: The equilibrium parameters estimated by the MCOD algorithm for the four fermentation broth concentrations.

Parameters	Fermentation broth concentration (% (v/v))			
	100	50	20	0
q_{max} (g g^{-1})	0.129	0.150	0.120	0.912
n	0.430	0.548	0.674	0.358
K_D (g^n l^{-n})	1.73	1.65	0.98	12.01
R^2	0.873	0.929	0.713	0.905

Table 2: The kinetic parameters estimated by the MCOD algorithm for the four fermentation broth concentrations.

Parameters	Fermentation broth concentration (% (v/v))			
	100	50	20	0
TM model				
k_1 (l g^{-1} h^{-1})	1.1 ± 0.2	3.6 ± 0.2	25.7 ± 0.3	18.7 ± 0.3
R^2	0.757	0.843	0.673	0.660
RSFK model				
k_1 (10^{-2} l g^{-1} h^{-1})	5.83 ± 0.02	9.172 ± 0.008	15.964 ± 0.009	40.01 ± 0.06
k_2 (10^{-2} h^{-1})	6.62 ± 0.02	10.265 ± 0.009	7.775 ± 0.009	1.93 ± 0.06
R^2	0.978	0.992	0.990	0.941
RNFK model				
k_1 (10^{-2} l^n g^{-n} h^{-1})	4.97 ± 0.03	7.62 ± 0.01	13.96 ± 0.02	3.3 ± 0.1
k_2 (10^{-1} h^{-1})	3.29 ± 0.03	3.97 ± 0.01	2.83 ± 0.02	17.4 ± 0.1
R^2	0.969	0.986	0.984	0.895
FPDM model				
D_l (10^{-12} m^2 s^{-1})	0.88 ± 0.02	1.173 ± 0.006	1.45 ± 0.01	1.48 ± 0.01
R^2	0.976	0.993	0.988	0.990
HSDM model				
D_l (10^{-14} m^2 s^{-1})	2.94 ± 0.01	1.6887 ± 0.0009	0.9494 ± 0.007	3.78 ± 0.05
R^2	0.987	0.999	0.994	0.947
MPM model				
D_l (10^{-14} m^2 s^{-1})	2.34 ± 0.02	3.141 ± 0.006	3.408 ± 0.009	1.81 ± 0.02
R^2	0.984	0.994	0.990	0.984
MPMPSD model				
D_l (10^{-14} m^2 s^{-1})	2.13 ± 0.01	3.735 ± 0.004	4.76 ± 0.01	1.30 ± 0.01
R^2	0.985	0.996	0.991	0.990
BPM model				
D_l (10^{-11} m^2 s^{-1})	2.53 ± 0.02	0.956 ± 0.005	1.629 ± 0.007	2.84 ± 0.07
D_μ (10^{-17} m^2 s^{-1})	0.47 ± 0.02	2.950 ± 0.005	1.504 ± 0.006	1.46 ± 0.07
R^2	0.976	0.995	0.993	0.923

Amongst these parameters, the one that deserves more attention is the effective diffusivity, beside the kinetic parameters of the non-structural TM, RSFK, and RNFK models, because of its impact on the concentration distributions. The effective diffusivities calculated by Quek and Al-Duri (2007) were $0.9–2.0 \times 10^{-9}$ m^2 s^{-1} and $0.7–1.0 \times 10^{-9}$ m^2 s^{-1} for the adsorption of Cu^{2+} and Pb^{2+}, respectively (FPDM model). The estimation method used was the same as that presented by Dadwhal *et al.* (2009), determining an effective diffusivity of $0.2–1.0 \times 10^{-14}$ m^2 s^{-1} (HSDM model) and $0.5–1.0 \times 10^{-10}$ m^2 s^{-1} (BPM model) for the adsorption of As^{5+}. This estimation method provided an accuracy of about 13–27% (Quek and Al-Duri, 2007). The results from the first mentioned work are different from those presented by Dadwhal *et al.* (2009), but if the accuracy of the estimation method is considered, the parameters estimated by the MCOD algorithm are in agreement with the published data taking into account that vancomycin molecule is larger than the metal ions mentioned. Initially, the parameters presented by Dadwhal *et al.* (2009) and Quek and Al-Duri (2007) were tested, but the results were not satisfactory.

Batch Experiments

Concentration Decrease Studies

The applicability of the previously validated models was demonstrated by the optimization of the adsorption process in the batch vessels in terms of two process efficiencies (Equations (35) and (36)).

$$\varphi_{90\%} = \frac{0.9t_{C/C_0=0.9}}{\int_0^{t_{C/C0=0.9}} C/C_0 dt} \quad (35)$$

$$\varphi_{10\%} = \frac{0.1t_{C/C_0=0.1}}{\int_0^{t_{C/C0=0.1}} C/C_0 dt} \quad (36)$$

Figure 1 shows the results of process simulation for vancomycin adsorption according to the proposed models, with the estimated parameters presented in Tables 1 and 2. The predicted concentration distributions fitted the experimental data well, some more than others, the validation step of the model having a COD higher than 0.95 for all FB concentrations, which applies to the FPDM, MPM, and MPMPSD models. The good performance of the models is confirmed in Table 3, where the two process efficiencies predicted by the model are compared with the experimental data for all the fermentation broth concentrations. This indicates that the model predictions are reliable and can be used as a tool for process optimization. For the fermentation broth concentrations of 0, 20, 50, and 100% (v/v) (C_0=4.96 , 1.17, 2.78, and 5.54 g L^{-1}, respectively) the experimental process efficiencies for concentration distributions up to $C/C_0 = 10\%$ and $C/C_0 = 90\%$ agreed best with the ones predicted by MPMPSD model.

In order to quantify the sensitivity of the model predictions with respect to the estimated parameter errors, a sensitivity analysis was performed. The values of the parameters for a FB concentration of 100% (v/v) (Table 1 and 2) were taken as the nominal values. The process model was solved assuming a relative parameter deviation ranging from −15% to +15% of the nominal values (Table 4). To quantify the deviation caused by the parameter increase/decrease, the process efficiency was calculated according to Equation (35) and compared with the nominal values (depending on the model; Table 3). Since all models utilized were deterministic and were solved using finite difference methods, they always produce the same output from a given starting condition or initial state. Hence, a fixed level of perturbations can be applied in order to observe the dependence of the process efficiency on parameter variation that may occur for various reasons, e.g., a variation in FB concentration.

Table 3: Experimental and predicted efficiencies for vancomycin adsorption in a batch vessel.

	Efficiency	Fermentation broth (FB) concentration (% (v/v))			
		100	50	20	0
Experimental	$\phi_{90\%}^{exp}$ (%)	94.7	94.7	94.7	94.7
	$\phi_{10\%}^{exp}$ (%)	35.2	35.6	27.4	37.7
TM model	$\phi_{90\%}^{cal}$ (%)	94.5	94.5	94.5	94.5
	$\phi_{10\%}^{cal}$ (%)	46.5	46.5	46.5	46.5
RSFK model	$\phi_{90\%}^{cal}$ (%)	94.2	93.7	93.2	89.3
	$\phi_{10\%}^{cal}$ (%)	29.4	27.8	26.6	26.1
RNFK model	$\phi_{90\%}^{cal}$ (%)	94.3	93.8	93.3	89.7
	$\phi_{10\%}^{cal}$ (%)	26.2	25.0	24.3	21.3
FPDM model	$\phi_{90\%}^{cal}$ (%)	91.0	88.4	83.6	82.9
	$\phi_{10\%}^{cal}$ (%)	50.5	52.1	54.5	49.7
HSDM model	$\phi_{90\%}^{cal}$ (%)	94.0	93.5	93.4	89.8
	$\phi_{10\%}^{cal}$ (%)	31.2	30.7	29.5	26.5
MPM model	$\phi_{90\%}^{cal}$ (%)	90.4	90.3	91.0	86.8
	$\phi_{10\%}^{cal}$ (%)	29.2	28.4	27.9	31.9
MPMPSD model	$\phi_{90\%}^{cal}$ (%)	90.1	89.9	90.5	85.1
	$\phi_{10\%}^{cal}$ (%)	30.9	29.8	28.6	33.9
BPM model	$\phi_{90\%}^{cal}$ (%)	93.1	93.8	93.2	87.2
	$\phi_{10\%}^{cal}$ (%)	25.2	26.9	26.3	23.7

Table 4: Parametric sensitivity of the model parameters for FB concentration 100% (v/v).

Parameter	$\phi_{90\%}^{cal}$ (%)	
	−15%	+15%
TM model		
k_1 ($l\ g^{-1}\ h^{-1}$)	94.5	94.5
RSFK model		
q_{max} ($g\ g^{-1}$)	94.3	94.1
k_1 ($10^{-2}\ l\ g^{-1}\ h^{-1}$)	94.3	94.1
k_2 ($10^{-2}\ h^{-1}$)	94.2	94.2
RNFK model		
q_{max} ($g\ g^{-1}$)	94.4	94.2
k_1 ($10^{-2}\ l^n\ g^{-n}\ h^{-1}$)	94.3	94.2
k_2 ($10^{-1}\ h^{-1}$)	94.3	94.3
FPDM model		
q_{max} ($g\ g^{-1}$)	91.6	90.9
D_l ($10^{-12}\ m^2\ s^{-1}$)	91.6	91.1
HSDM model		
q_{max} ($g\ g^{-1}$)	94.3	93.9
D_l ($10^{-14}\ m^2\ s^{-1}$)	94.3	93.9
MPM model		
q_{max} ($g\ g^{-1}$)	91.9	89.4
D_l ($10^{-14}\ m^2\ s^{-1}$)	90.8	89.9
MPMPSD model		
q_{max} ($g\ g^{-1}$)	90.8	87.7
D_l ($10^{-14}\ m^2\ s^{-1}$)	90.5	89.4
BPM model		
q_{max} ($g\ g^{-1}$)	93.1	93.1
D_l ($10^{-11}\ m^2\ s^{-1}$)	93.4	92.9
D_μ ($10^{-17}\ m^2\ s^{-1}$)	93.1	93.1

The method and the fixed level of perturbations (−15% and +15%) were chosen following Moraes *et al*. (2009) for comparative reasons. Sensitivity analysis was executed after the optimal parameter values had been estimated (Table 2) and was thus completely independent of the regression analysis. Except for the BPM model, the most sensitive variable in the process was the maximum adsorbed amount and an increment increase/decrease in its value led to a noticeable increase/decrease in process efficiency. This reduction in efficiency is to be expected at low maximum adsorbed amount, since there is a decrease in the holding capacity for vancomycin. In practice, there should be a loss of dynamic binding capacity with increasing FB concentration, since there should be fewer vancomycin molecules in contact with the resin. This hypothesis is not confirmed by the experimental process efficiencies presented in Table 3, which were all 94.7% ($\phi_{90\%}^{exp}$) and 27.4−37.7% ($\phi_{10\%}^{exp}$), respectively. This may be explained by the fact that the adsorbent is in great excess compared to the active ingredient and the microorganisms combined. Therefore, the fractional coverage of the adsorbent surface is low enough so that there is no competition for empty surface sites between the active ingredient and microorganisms. The estimated TM, RSFK, RNFK, MPM, and MPMPSD model parameters for the adsorption(/desorption) kinetics presented in Table 2 show that, at higher/lower adsorption/ desorption parameter values, the efficiency ($\phi_{10\%}^{cal}$) decreases. This is probably due to the fact that higher/lower adsorption/desorption parameter values result in an initial fast and subsequent slow concentration decrease, causing lower $\phi_{10\%}^{cal}$, whereas the opposite applies for lower/higher adsorption/ desorption parameter values.

Forrer *et al.* (2008) showed that the maximum adsorbed amount of antibodies ranged from 286.7 mg $ml_{ads.}^{-1}$ to 287.5 mg $mL_{ads.}^{-1}$ for ionic strengths ranging from 0.07 M to 0.17 M. This suggests that the dynamic binding capacity does not necessarily change throughout the process because of the presence of a competing adsorption component. In the present work, however, the maximum adsorbed amount was estimated for each FB concentration separately and these individual (and not mean (Forrer *et al.*, 2008)) values were applied in the adsorption kinetic models. The increase in sensitivity of the maximum adsorbed amount is presumably due to its estimation from equilibrium experiments, whereas the parameters of the adsorption kinetics were obtained from transient experiments. In these situations, the accuracy of the model predictions is guaranteed by separate determination of equilibrium and kinetic parameters and the use of an efficient method of parameter estimation, the MCOD algorithm.

In the analyses of the process efficiencies (Table 3), except for the MPM, MPMPSD, and BPM model, the highest $\phi_{90\%}^{exp}$ efficiencies were obtained for the FB concentration of 100% (v/v) under the conditions specified. The same goes for $\phi_{10\%}^{exp}$, except for the FPDM and BPM models, the exceptions being attributed to experimental error. Nevertheless, this is not a sufficient argument to affirm that it is the best FB concentration for vancomycin separation in a batch vessel, since this may also depend on the processing time, which should be considered in the analysis. The elapsed times for the concentration distributions to reach the values that permitted the calculation of the two process efficiencies (Equations (35) and (36)) were 0.25 min, 2.73 min, 3.21 min, and 4.53 min ($\phi_{90\%}^{exp}$) and 21 min, 48 min, 103 min, and 182 min ($\phi_{10\%}^{exp}$ for FB concentrations of 0, 20, 50, and 100% (v/v), respectively. According to these results, the FB concentration of 0% (v/v) was the best for vancomycin

adsorption, since the times to reach 90% and 10% of initial concentration were 1/18 and 1/9 of those for the FB concentration of 100% (v/v), respectively.

In the present work, the model parameters were estimated for each fermentation broth concentration using only a single vancomycin concentration (4.96, 1.17, 2.78, and 5.54 g L^{-1}, respectively). Parameters were estimated for each individual FB vancomycin concentration, because it would be almost impossible to know the variation in concentration of all medium components (subsection Materials) upon FB dilution from 100% (v/v) to 0% (v/v). It was shown that different medium components, mostly microorganisms, may competitively adsorb to the particle surface (Likozar *et al.*, 2012) and decrease q_{max} (Table 1). Although statistically more significant results could be obtained by global analysis of all experimental data, the agreement with any model would be rather poor and definitively unrepresentative of the process. Thus, it is more favorable to perform the regression analysis for each FB concentration individually and interpolate the parameter values for a given FB concentration. The applicability of the model was demonstrated in the validation step, where COD was calculated to determine how well the model predictions agreed with the experimental data, as shown in Figure 1. Thus, the model was used to predict process performance under several experimental conditions. In continuation, however, a new methodology is proposed, since most of the works published so far on model development using chromatographic processes have considered mono- or bi-component systems (Bak *et al.*, 2007) and hardly any multi-component systems, like a fermentation broth (Mendieta-Taboada *et al.*, 2001) have been reported.

Effect of Changing the Batch Parameters

Process optimization (PO) was performed as follows. In a batch adsorption process, the main manipulable variables are the fermentation broth concentration (the liquid phase properties are implicit in the FB concentration), resin fraction $1-\varepsilon$ (this is implicated in the final concentration of vancomycin in the batch), and the initial concentration (C_0). As the parameters were estimated for each FB concentration, the only independent variables were $1-\varepsilon$ and C_0. To optimize this process, a sensitivity analysis for two independent variables was carried out for each FB concentration. The values of these independent variables are shown in Table 5.

Table 5: Table of the PO variable values with responses in terms of the process efficiencies for the four fermentation broth concentrations as predicted by the MPMPSD model.

$1-\varepsilon$ (/)	C_0 (g l^{-1})	$\phi_{90\%}^{cal}$ (%)				$\phi_{10\%}^{cal}$ (%)			
		100	50	20	0	100	50	20	0
0.01	10^{-2}	86.0	92.3	94.8	85.7	32.2	28.9	27.4	31.8
0.01	10^{-1}	94.3	95.4	95.4	88.7	29.2	27.9	29.1	31.4
0.01	10^{0}	96.5	96.0	95.7	96.5	/	/	/	/
0.01	10^{1}	96.5	96.2	96.1	96.6	/	/	/	/
0.01	10^{2}	/	/	/	/	/	/	/	/
0.25	10^{-2}	83.9	83.9	83.2	83.9	12.7	12.7	16.3	12.7
0.25	10^{-1}	83.9	83.4	86.8	83.9	12.7	15.1	27.0	12.7
0.25	10^{0}	85.8	86.5	88.1	83.5	31.0	30.1	28.7	15.4
0.25	10^{1}	87.8	90.4	91.4	86.0	31.5	29.9	29.2	33.1
0.25	10^{2}	96.3	95.5	95.1	95.7	31.4	29.1	28.7	29.6
0.50	10^{-2}	83.9	83.9	83.9	83.9	12.7	12.7	12.7	12.7
0.50	10^{-1}	83.9	83.9	83.6	83.9	12.7	12.7	15.4	12.7
0.50	10^{0}	83.9	83.4	85.3	83.9	12.7	14.6	24.3	12.7
0.50	10^{1}	85.1	86.6	87.6	83.2	32.8	30.5	29.0	28.8
0.50	10^{2}	90.5	90.4	90.3	88.1	30.7	30.2	30.2	31.9
0.75	10^{-2}	84.0	84.0	84.0	83.9	12.7	12.7	12.7	12.7
0.75	10^{-1}	84.0	84.0	84.0	83.9	12.7	12.7	12.7	12.7
0.75	10^{0}	84.0	84.0	84.0	83.9	12.7	12.7	12.7	12.7
0.75	10^{1}	83.9	83.6	86.1	83.9	12.4	15.0	17.7	12.7
0.75	10^{2}	86.8	86.8	86.6	85.3	33.9	31.9	30.7	33.8
0.99	10^{-2}	85.7	87.1	88.1	85.4	13.0	13.2	13.4	12.9
0.99	10^{-1}	85.7	87.1	88.1	85.4	13.0	13.2	13.4	12.9
0.99	10^{0}	85.7	87.1	88.1	85.4	13.0	13.2	13.4	12.9
0.99	10^{1}	85.7	87.1	88.1	85.4	13.0	13.2	13.4	12.9
0.99	10^{2}	85.7	87.1	88.1	85.4	13.0	13.2	13.4	12.9

The best validated model (MPMPSD) was used to simulate the process for different resin fractions and initial vancomycin concentrations, using a wide range of both variables for optimization. Table 5 presents the results in terms of the computed efficiencies for the five values of each variable, with a total of 25 runs. It should be noted that, in Table 5, the runs for the resin fraction of 0.25 and the initial vancomycin concentration of 10^2 g L^{-1} for both 0 and 100% (v/v) FB concentration provided similar results and were the best for all FB concentrations in terms of the summation of the two process efficiencies. The FB concentration of 20% (v/v) showed the highest efficiencies in the majority of runs. In general both efficiencies increased with the initial vancomycin concentration.

The data in Table 5 may thus be used to determine the effects of each independent variable on the efficiencies. Moreover, the initial concentration is usually connected to the FB concentration, i.e., the same FB should always yield the same amount of the active ingredient during fermentation and the latter is considered to be the initial adsorption process concentration. Consequently, the impact of FB concentration on the adsorption rate had to be considered in the dependency of adsorption kinetic parameters (Table 2) on FB concentration. These effects, represented by bar charts, are shown in Figure 2. The most significant positive or negative effects (maximal (MAX) or minimal (MIN) parameter value) on the kinetic parameters were between 6 and 51% (v/v) of the FB concentration, and the FB concentration of about 20% (v/v) can be considered optimal as far as adsorption kinetics are concerned. This tendency was predominant for both structural (FPDM, HSDM, MPM, MPMPSD, and BPM) and non-structural (TM, RSFK, and RNFK) models.

A more detailed analysis of both efficiencies was performed in order to validate the results, which are represented in Table 5 in terms of the calculated efficiencies. In a typical experiment, the assumption is that the C_0 value differentiates between the concentrations of 1 and 10 g L^{-1}. In this study, all concentrations were within this range. The resin fractions used for the more detailed calculation of efficiencies presented in Figures 3 and 4 varied from about 1.8 times greater to 1.6 times lower than the experimental ones, demonstrating a wide enough optimization range and allowing the construction of the plots presented as Figures 3 and 4.

The plots of the process efficiencies for the four fermentation broth concentrations are presented in Figures 3 and 4. In all cases, the maximum efficiencies $\phi_{10\%}^{cal}$ were obtained at the lowest levels of the resin fraction and the highest levels of initial vancomycin concentration, whereas the maximum efficiencies $\phi_{90\%}^{cal}$ were obtained at different levels of the resin fraction and initial vancomycin concentration. Since the goal was to select a common plot region where the efficiency was the highest for the process, it was necessary to define the range of each independent variable that led to maximum efficiency.

Although a FB concentration 20% (v/v) led to the most kinetically efficient vancomycin adsorption in the batch vessel, the elapsed process time was about 2−11 times longer than that for the FB concentration of 0% (v/v). Since the process efficiency was at best only 14% higher than that for the FB concentration of 0% (v/v), and sometimes even lower than the latter, this condition would not necessarily be of interest from an industrial point of view. Between the FB concentrations 50 and 100% (v/v), the latter showed the best results, mainly for the process efficiency $\phi_{10\%}^{cal}$.

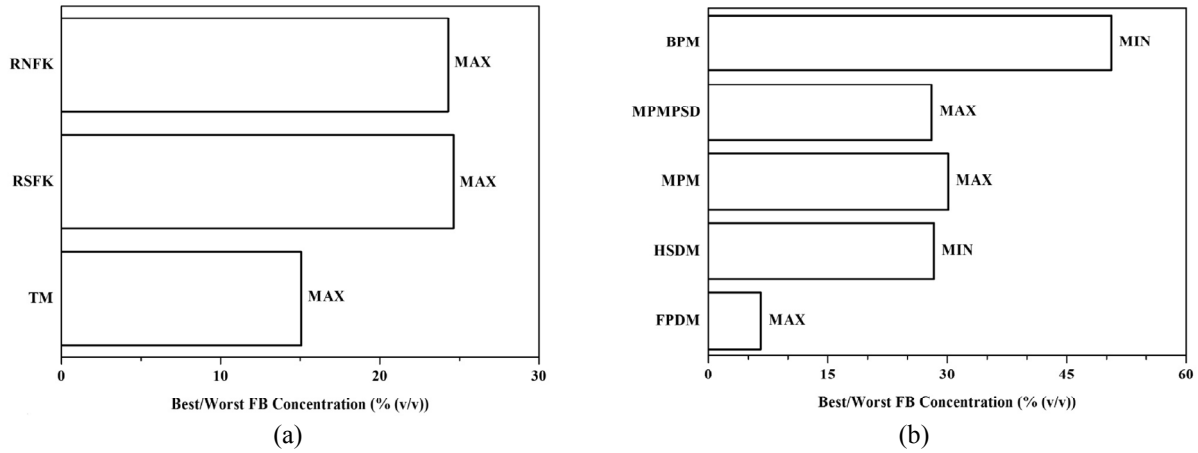

Figure 2: Bar chart for the PO. (a) Best/worst FB concentrations calculated from the adsorption kinetics parameter k_1; (b) Best/worst FB concentrations calculated from the adsorption kinetics parameter D_l.

Industrially, the process efficiency $\phi_{90\%}^{cal}$ is more important than $\phi_{10\%}^{cal}$, since for valuable products (as in the case of antibiotics) it is unlikely that the adsorbent batch will be loaded up to its total capacity, because the loss in antibiotic would increase the purification costs (Chang and Chase, 1996). Considering this fact, a FB concentration of 20% (v/v) represents the most promising option for vancomycin purification, since the process efficiencies were as high as 96% ($\phi_{90\%}^{cal}$) and 31% ($\phi_{10\%}^{cal}$). Moreover, the value of the superficial rotational velocity was also shown not to influence the process, allowing neglect of mass transfer resistance and an increase in process productivity.

The maximum efficiencies were observed at resin fraction values below 0.25 and for the extreme value of vancomycin concentration (100 g L^{-1}) for all the fermentation broth concentrations. Considering the cost of the resin, it is more advantageous to operate with the lowest resin weight possible. Thus, in the present work, the minimum fraction was defined as 0.25 for future simulations because, at the resin fraction of 0.01, the active ingredient concentration remained above $C/C_0 = 10\%$. The analysis of the FB concentration effects (Figure 2) showed that a dilution of the initial fermentation broth had a positive effect on the adsorption rate. The maximum vancomycin concentration obtained by fermentation for this strain was 5.54 g L^{-1}. Thus, the simulations were only carried out at 1−10 g L^{-1} with resin fractions of 0.5−0.9 for all FB concentrations.

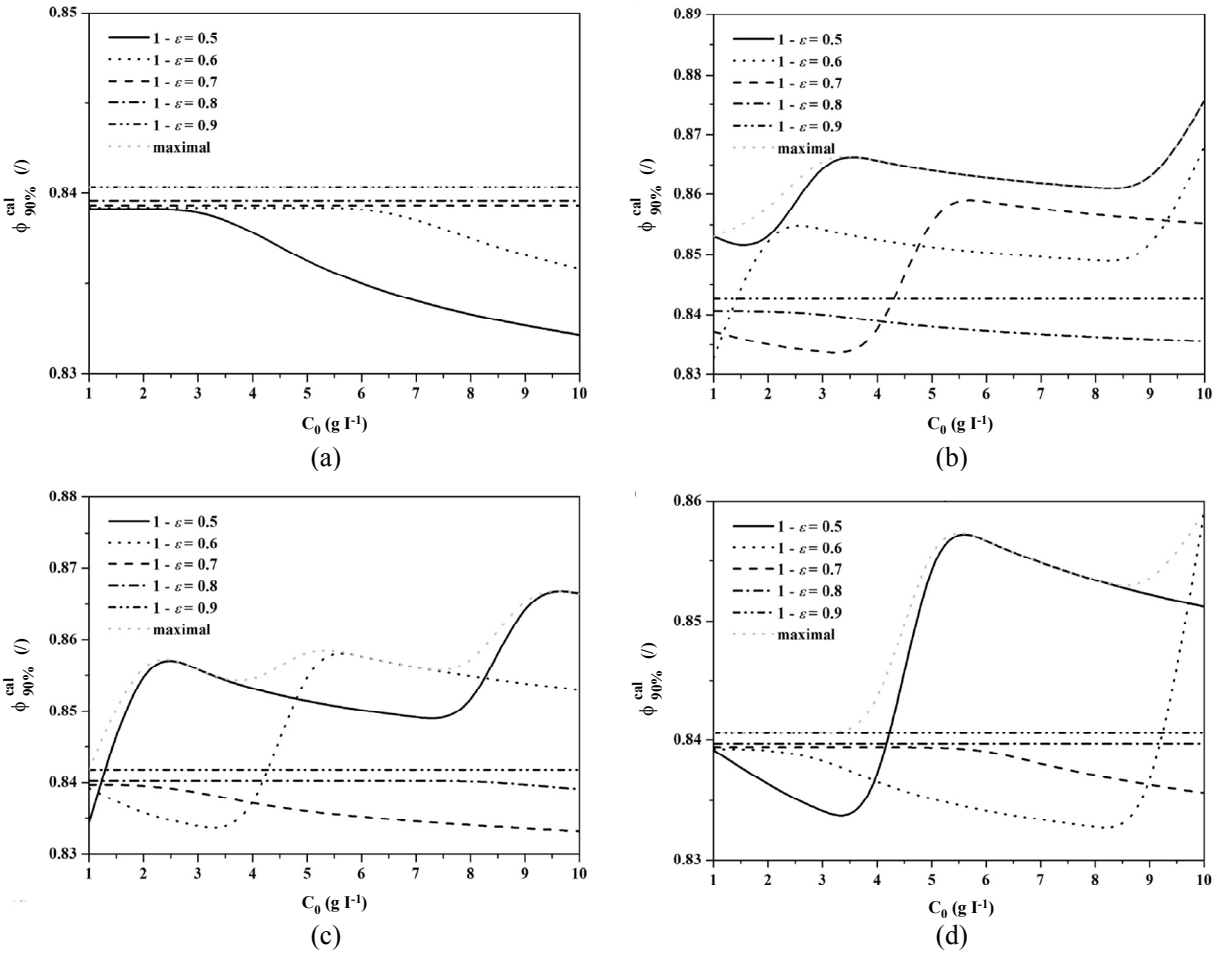

Figure 3: Plot for the PO. (a) Process efficiency $\phi_{90\%}^{cal}$ for the FB concentration 0% (v/v); (b) process efficiency $\phi_{90\%}^{cal}$ for the FB concentration 20% (v/v); (c) process efficiency $\phi_{90\%}^{cal}$ for the FB concentration 50% (v/v); (d) process efficiency $\phi_{90\%}^{cal}$ for the FB concentration 100% (v/v).

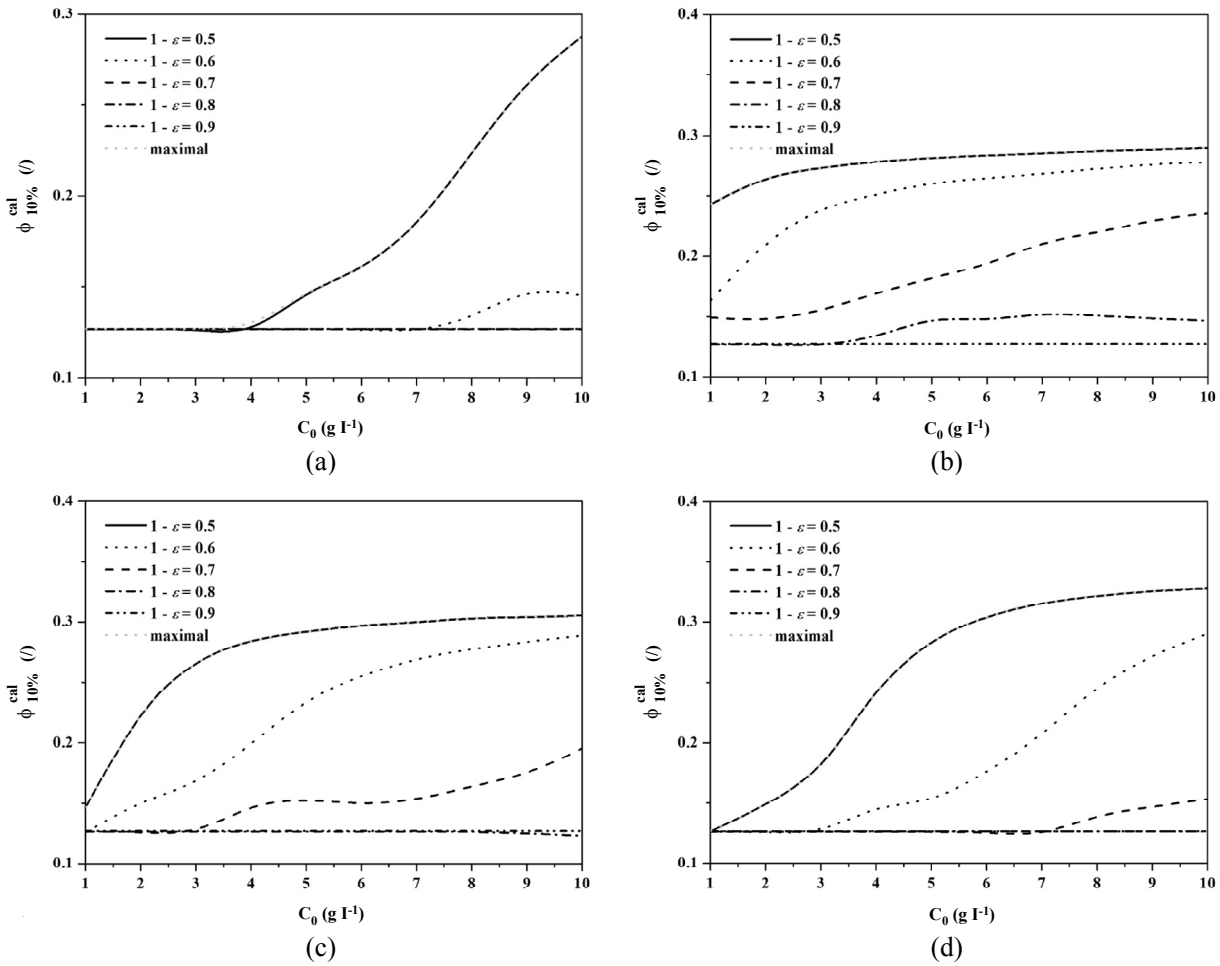

Figure 4: Plot for the PO. (a) Process efficiency $\phi^{cal}_{10\%}$ for the FB concentration 0% (v/v); (b) process efficiency $\phi^{cal}_{10\%}$ for the FB concentration 20% (v/v); (c) process efficiency $\phi^{cal}_{10\%}$ for the FB concentration 50% (v/v); (d) process efficiency $\phi^{cal}_{10\%}$ for the FB concentration 100% (v/v).

The process efficiencies $\phi^{cal}_{90\%}$ for initial vancomycin concentrations of 1−10 g l^{-1} were practically the same (84.0%-84.3% for all FB concentrations) for the resin fraction of 0.9, as were the process efficiencies $\phi^{cal}_{10\%}$ (12.7% for all FB concentrations), leading to the conclusion that this process is very robust under certain conditions (high resin fraction). In bioprocesses, robust situations are highly advantageous, since the antibiotic concentrations from microbial fermentations may not always be the same.

CONCLUSIONS

The focus of this study was active ingredient (vancomycin) adsorption during batch experiments. The variables examined in this study included the initial fermentation broth concentration, the initial vancomycin concentration, the volume fraction of adsorbent particles, and the rotation rate. The adsorption behavior was characterized in terms of the vancomycin concentration at the end of the process in the equilibrium state, as well as at various times during the process, as a function of the fermentation broth concentration in the batch vessel. Key batch characteristics were the two process efficiencies, defined as the times when the batch concentration was equal either to 90% or 10% of the initial concentration. The experimental results showed that the first efficiency ($\phi^{exp}_{90\%}$) did not change upon increasing the fermentation broth concentration, while the second efficiency ($\phi^{exp}_{10\%}$) was the best for the fermentation broth supernatant. Both calculated efficiencies increased upon

increasing the initial ingredient concentration in a batch and decreased upon increasing the initial fraction of adsorbent. It was also observed that, as the initial fermentation broth concentration decreased, the kinetic performance improved significantly and the process times decreased.

Eight adsorption models (TM, RSFK, RNFK, FPDM, HSDM, MPM, MPMPSD and BPM) were applied to the batch experiments. All models predicted the qualitative trends quite well. The coefficient of correlation (COD) (also known as the Pearson product−moment correlation coefficient, PMCC) was used to compare the eight models with respect to their ability to fit the experimental data. Overall, the MPMPSD provided the best fit (the highest sum of COD) due to its consideration of the particle size distribution and not just their mean size; in all cases, the TM was the worst due to its simplicity.

Future work will include scale-up of batch experiments and modeling at the industrial expanded-bed column level, where hydrodynamic effects will probably not be negligible and will indirectly influence mass transfer in the liquid film around the adsorbent particles. Regardless of this, the developed models are readily usable for the optimization of different fermentation broths with varying active ingredients in order to improve the process and thus economic productivity, provided that the essential model parameters can be determined beforehand.

ACKNOWLEDGEMENT

The authors acknowledge the support of Slovenian Research Agency (Program P2−0152), student Đorđe Lovrić and Development of Anti-Infectives, Department of Microbiology and Fermentations, Lek d.d., a Sandoz company, in this work, especially the experimental support.

NOMENCLATURE

C	active ingredient mass concentration in the liquid phase	kg m^{-3}
C_0	initial active ingredient mass concentration in the liquid phase	kg m^{-3}
C^*	equilibrium active ingredient mass concentration in the liquid phase	kg m^{-3}
C_m	active ingredient mass concentration in pore phase	kg m^{-3}
$C_{m,i}$	active ingredient mass concentration in the ith fraction pore phase	kg m^{-3}
COD	coefficient of determination	/
D_b	active ingredient molecular diffusion coefficient	m^2 s^{-1}
D_l	active ingredient effective diffusion coefficient	m^2 s^{-1}
D_μ	active ingredient effective diffusion coefficient in the micro-particle	m^2 s^{-1}
f	probability density function of radius of the solid phase particle	m^{-1}
J	Jacobian matrix	/
k_1	active ingredient adsorption rate constant	kg^{-n} m^{3n} s^{-1}
k_2	active ingredient desorption rate constant	s^{-1}
K_D	active ingredient adsorption equilibrium constant reciprocal	kg^n m^{-3n}
$\dot{m}$	active ingredient mass transfer rate	kg s^{-1}
n	active ingredient adsorption order	/
N	number of measurements	/
p	number of parameters	/
q	mass of active ingredient per solid phase mass	/
$\overline{q}$	average mass of active ingredient per solid phase mass	/
q^*	equilibrium mass of active ingredient per solid phase mass	/
$\overline{q}_i$	average mass of active ingredient per ith fraction solid phase mass	/
q_i^*	equilibrium mass of active ingredient per ith fraction solid phase mass	/
$\overline{q}_\mu$	average mass of active ingredient per solid micro-particle mass	/
q_{max}	maximal equilibrium mass of active ingredient per solid phase mass	/
r	radius	m
r_f	radius of un-adsorbed solid phase in a particle	m

R_p	radius of solid phase particle	m
$R_{p,i}$	minimal radius of i^{th} fraction solid phase particles	m
$R_{p,i}^{average}$	average radius of i^{th} fraction solid phase particles	m
$R_{p,max}$	maximal radius of 98.0% solid phase particles	m
R_p^{mean}	mean radius of solid phase particle	m
$R_{p,min}$	minimal radius of 98.0% solid phase particles	m
R_μ	radius of micro-particle	m
r_μ	radius within micro-particle	m
t	time	s
y	vector of measured values	kg m^{-3}
$\overline{y}$	average measured value	kg m^{-3}
y^{calc}	vector of calculated values	kg m^{-3}
$\overline{y}^{calc}$	average calculated value	kg m^{-3}
y_i^{calc}	component of vector of calculated values	kg m^{-3}
y_i	component of vector of measured values	kg m^{-3}

Greek Letters

Γ	tortuosity	/
ε	volume fraction of liquid phase	/
ε_m	volume fraction of pore phase	/
σ	standard deviation	variable
σ_s	radius of solid phase particle standard deviation	m
ρ	density of solid phase	kg m^{-3}
$\phi_{10\%}$	calculated 90% adsorption efficiency	/
$\phi_{90\%}$	calculated 10% adsorption efficiency	/
$\phi_{10\%}^{exp}$	measured 90% adsorption efficiency	/
$\phi_{90\%}^{exp}$	measured 10% adsorption efficiency	/
ω_r	angular velocity	s^{-1}

REFERENCES

Ansari, S. A., Mohapatra, P. K. and Manchanda, V. K., A novel malonamide grafted polystyrene-divinyl benzene resin for extraction, pre-concentration and separation of actinides. Journal of Hazardous Materials, 161, No. 2-3, 1323 (2009).

Bak, H., Thomas, O. R. T. and Abildskov, J., Lumped parameter model for prediction of initial breakthrough profiles for the chromatographic capture of antibodies from a complex feedstock. Journal of Chromatography, B 848, No. 1, 131 (2007).

Borin, B. and Pavko, A., Adsorption of vancomycin on AMBERLITE XAD-16 in a packed bed column. Chemical and Biochemical Engineering Quarterly, 23, No. 4, 479 (2009).

Brauch, V. and Schlünder, E. U., The scale-up of activated carbon columns for water purification, based on results from batch tests. 2. Theoretical and experimental determination of breakthrough curves in activated carbon columns. Chemical Engineering Science, 30, No. 5-6, 539 (1975).

Burkert, J. F. M., Kalil, S. J., Maugeri, F. and Rodrigues, M. I., Parameters optimization for enzymatic assays using experimental design. Brazilian Journal of Chemical Engineering, 23, No. 2, 163 (2006).

Cen, P. L. and Yang, R. T., Analytic solutions for adsorber breakthrough curves with bidisperse sorbents (zeolites). AIChE Journal, 32, No. 10, 1635 (1986).

Chang, Y. K. and Chase, H. A., Development of operating conditions for protein purification using expanded bed techniques: The effect of the degree of bed expansion on adsorption performance. Biotechnology and Bioengineering, 49, No. 5, 512 (1996).

Dadwhal, M., Ostwal, M. M., Liu, P. K. T., Sahimi, M. and Tsotsis, T. T., Adsorption of arsenic on conditioned layered double hydroxides: Column experiments and modeling. Industrial & Engineering Chemistry Research, 48, No. 4, 2076 (2009).

Du, X., Yuan, Q., Zhao, J. and Li, Y., Comparison of general rate model with a new model - artificial neural network model in describing chromatographic kinetics of solanesol adsorption in packed column by macroporous resins. Journal of Chromatography A, 1145, No. 1-2, 165 (2007).

Forrer, N., Butté, A. and Morbidelli, M., Chromatographic behavior of a polyclonal antibody mixture on a strong cation exchanger column. Part II: Adsorption modeling. Journal of Chromatography A, 1214, No. 1-2, 71 (2008).

Gottipati, R. and Mishra, S., Application of biowaste (waste generated in biodiesel plant) as an adsorbent for the removal of hazardous dye − methylene blue − from aqueous phase. Brazilian Journal of Chemical Engineering, 27, No. 2, 357 (2010).

Han, R., Wang, Y., Zou, W., Wang, Y. and Shi, J., Comparison of linear and nonlinear analysis in

estimating the Thomas model parameters for methylene blue adsorption onto natural zeolite in fixed-bed column. Journal of Hazardous Materials, 145, No. 1-2, 331 (2007).

Kumar, P. S., Kirthika, C. V. K. and Kumar, K. S., Kinetics and equilibrium studies of Pb^{2+} ion removal from aqueous solutions by use of nano-silversol-coated activated carbon. Brazilian Journal of Chemical Engineering, 27, No. 2, 339 (2010).

Likozar, B., Senica, D. and Pavko, A., Equilibrium and kinetics of vancomycin adsorption on polymeric adsorbent. AIChE Journal, 58, No. 1, 99 (2012).

Levenspiel, O., Chemical Reaction Engineering. Wiley, New York (1999).

McIntyre, J. J., Bull, A. T. and Bunch, A. W., Vancomycin production in batch and continuous culture. Biotechnology and Bioengineering, 49, No. 4, 412 (1996).

Mendieta-Taboada, O., Kamimura, E. S. and Maugeri, F., Modelling and simulation of the adsorption of the lipase from *Geotrichum* sp on hydrophobic interaction columns. Biotechnology Letters, 23, No. 10, 781 (2001).

Moraes, C. C., Mazutti, M. A., Rodrigues, M. I., Maugeri, F. and Kalil, S. J., Mathematical modeling and simulation of inulinase adsorption in expanded bed column. Journal of Chromatography A, 1216, No. 20, 4395 (2009).

Papini, M. P., Kahie, Y. D., Troia, B. and Majone, M., Adsorption of lead at variable pH onto a natural porous medium: Modeling of batch and column experiments. Environmental Science & Technology, 33, No. 24, 4457 (1999).

Piccin, J. S., Dotto, G. L. and Pinto, L. A. A., Adsorption isotherms and thermochemical data of FD&C Red N° 40 binding by Chitosan. Brazilian Journal of Chemical Engineering, 28, No. 2, 295 (2011).

Quek, S. Y. and Al-Duri, B., Application of film-pore diffusion model for the adsorption of metal ions on coir in a fixed-bed column. Chemical Engineering and Processing, 46, No. 5, 477 (2007).

Spahn, H. and Schlünder, E. U., The scale-up of activated carbon columns for water purification, based on results from batch tests. 1. Theoretical and experimental determination of adsorption rates of single organic solutes in batch tests. Chemical Engineering Science, 30, No. 5-6, 529 (1975).

Thomas, H. C., Heterogeneous ion exchange in a flowing system. Journal of the American Chemical Society, 66, No. 10, 1664 (1944).

Tian, Q., Gomersall, C. D., Leung, P. P. N., Choi, G. Y. S., Joynt, G. M., Tan, P. E. and Wong, A. S. Y., In vitro adsorption of vancomycin by three types of hemofilters. Critical Care Medicine, 34, No. 12, A97 (2006).

Tian, Q., Gomersall, C. D., Leung, P. P. N., Choi, G. Y. S., Joynt, G. M., Tan, P. E. and Wong, A. S. Y., The adsorption of vancomycin by polyacrylonitrile, polyamide, and polysulfone hemofilters. Artificial Organs, 32, No. 1, 81 (2008).

Von Winckelmann, S., Laleman, W., Willems, L. and Indevuyst, C., Influence of the molecular adsorbents recirculating system (MARS) on serum levels of vancomycin, tacrolimus, and mycophenolate mofetil. Pharmacy World & Science, 31, No. 2, 267 (2009).

Yagi, S. and Kunii, D., Fluidized-solids reactors with continuous solids feed − II: Conversion for overflow and carryover particles. Chemical Engineering Science, 16, No. 3-4, 372 (1961).

Yan, H. S., Zhao, Q. X., Yuan, J., Cheng, X. H. and He, B. L., Affinity adsorbents for the vancomycin group of antibiotics. Biotechnology and Applied Biochemistry, 31, No. 1, 15 (2000).

Yang, L., Dadwhal, M., Shahrivari, Z., Ostwal, M. M., Liu, P. K. T., Sahimi, M. and Tsotsis, T. T., Adsorption of arsenic on layered double hydroxides: Effect of the particle size. Industrial & Engineering Chemistry Research, 45, No. 13, 4742 (2006).

Yuan, J., Xu, J. J., Niu, W. Q., Zhao, Q. X., Yan, H. S., Cheng, X. H. and He, B. L., Affinity adsorbents with D-alanine and D,L-alanine as ligands for vancomycin group antibiotics. Journal of Liquid Chromatography & Related Technologies, 24, No. 17, 2635 (2001).

Yun, J. X., Yao, S. J., Lin, D. Q., Lu, M. H. and Zhao, W. T., Modeling axial distributions of adsorbent particle size and local voidage in expanded bed. Chemical Engineering Science, 59, No. 2, 449 (2004).

Zabka, M., Minceva, M. and Rodrigues, A. E., Experimental and modeling study of adsorption in preparative monolithic silica column. Chemical Engineering and Processing, 45, No. 2, 150 (2006).